Front. Phys. 13(2), 137203 (2018)
https://doi.org/10.1007/s11467-017-0744-0

RESEARCH ARTICLE

Electron drift velocity and mobility in graphene

Hai-Ming Dong[1], **Yi-Feng Duan**[1,†], **Fei Huang**[2,3,‡], **Jin-Long Liu**[3]

[1] *School of Physical Science and Technology, China University of Mining and Technology, Xuzhou 221116, China*
[2] *Low Carbon Energy Institute, China University of Mining and Technology, Xuzhou 221116, China*
[3] *School of Materials Science and Engineering, China University of Mining and Technology, Xuzhou 221116, China*
Corresponding authors. E-mail: [†]*yifeng@cumt.edu.cn,* [‡]*huangfei7804@163.com*
Received July 26, 2017; accepted November 22, 2017

We present a theoretical study of the electric transport properties of graphene-substrate systems. The drift velocity, mobility, and temperature of the electrons are self-consistently determined using the Boltzmann equilibrium equations. It is revealed that the electronic transport exhibits a distinctly nonlinear behavior. A very high mobility is achieved with the increase of the electric fields increase. The electron velocity is not completely saturated with the increase of the electric field. The temperature of the hot electrons depends quasi-linearly on the electric field. In addition, we show that the electron velocity, mobility, and electron temperature are sensitive to the electron density. These findings could be employed for the application of graphene for high-field nano-electronic devices.

Keywords graphene, mobility, nano-electronic devices

PACS numbers 72.80.Vp, 81.05.ue, 73.63.-b

1 Introduction

Graphene, a monolayer of carbon atoms with a dense honeycomb two-dimensional structure, was demonstrated by Geim's research group in 2004 [1]. Such linear-energy-dispersion gapless Dirac systems have attracted increasing research interests in condensed matter physics, nanomaterials science, and nano-electronic devices. In particular, graphene-wafer systems, whose carrier density can be effectively controlled through the gate voltage, exhibit excellent electronic transport properties including high mobility [2], long mean free path [3], and high on/off current ratio [4]. Graphene has already been employed to develop novel nano-electronic devices, including field-effect transistors (FETs) [5], p-n junctions [6], and high-frequency devices [7]. The transport properties of graphene are an important research topic owing to the significant potentials for nano-device applications [8].

Recently, several experimental studies were focused on the electric transport properties of graphene at high electric fields [9, 10]. It was experimentally revealed that the carrier mobilities of graphene-FETs significantly exceed the universal mobilities of silicon FETs and ultra-thin metal-oxide-semiconductor devices [9]. Furthermore, it was experimentally indicated that at room temperature, a gated graphene device exhibits a very high carrier density and source-drain (SD) current density, along with unusual current–voltage characteristics [10, 11]. For graphene, the SD current saturates when the SD voltage V_{SD} reaches a value of several volts [10], while the I–V characteristics exhibit a strongly non-linear/non-ohmic behavior [10, 11]. It is worth noting that the current saturation is incomplete and sensitive to the carrier density of the graphene samples (i.e., to the applied gate voltage) [11]. These experimental findings suggest that graphene can be employed in the development of advanced high-field high-speed nano-electronic devices. Motivated by the above experimental findings, we performed a theoretical study on the electric transport properties of graphene.

2 Theoretical approach

In this study, we consider a gate-controlled graphene device on a dielectric wafer (Fig. 1), e.g., SiO_2/Si, similar to the experimental devices [4, 9, 11]. In such systems, the carrier (electron or hole) density can be effectively tuned by the applied gate voltage V_g. In addition, an in-plane electron velocity and mobility can be induced by

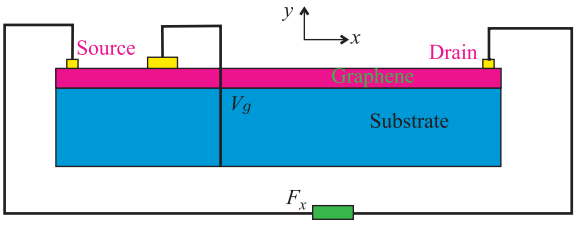

Fig. 1 Schematic of the graphene-Si/SiO_2-substrate-wafer system in the presence of a DC electric field F_x and gate voltage V_g.

the source-to-drain DC electric field F_x, applied along the x-direction of the graphene sheet [11, 12]. The carriers of a monolayer graphene at low energies can be described by the Weyl's equation; the wave-function $\psi_{\lambda \boldsymbol{k}}(\boldsymbol{r}) = 2^{-1/2}[1, \lambda e^{i\phi}]$ and energy spectrum $E_\lambda(\boldsymbol{k}) = \lambda\hbar v_F|\boldsymbol{k}|$ can be obtained analytically [13], where $r = (x, y)$, $\boldsymbol{k}$ is the wave-vector of an electron or hole along the graphene sheet, $v_F = 10^8$ cm/s is the Fermi-velocity, ϕ is the angle between $\boldsymbol{k}$ and x-direction, while $\lambda = +1$ for an electron and $\lambda = -1$ for a hole.

We employ the semi-classical Boltzmann equation (BE), developed by Lei [14], to study the response of the carriers in graphene to the applied DC driving electric field with a strength of F_x. The usual balance-equation approach based on the BE is employed to investigate the electric transport properties of the considered graphene systems [14, 15]. Next, we assume that, in the presence of a positive gate voltage, the conducting carriers in graphene are electrons. For the first moment, the momentum-balance equation can be derived for the electrons:

$$eF_x n_e/\hbar = M_{\rm ei} + M_{\rm ea} + M_{\rm eo}, \tag{1}$$

$$M_{\rm ei} = \frac{2}{\pi^3\gamma}\int_0^\infty {\rm d}k \int_0^{2\pi} {\rm d}\phi \int_0^{2\pi} {\rm d}\theta k k'[k\cos\phi - k'\cos(\phi+\theta)] f_+(k)|U_{\rm ei}|^2,$$

$$M_{\rm ea} = \frac{2}{\pi^3\gamma}\int_0^\infty {\rm d}k \int_0^{2\pi} {\rm d}\phi \int_0^{2\pi} {\rm d}\theta k k'[k\cos\phi - k'\cos(\phi+\theta)] f_+(k)|U_{\rm ea}|^2,$$

and

$$M_{\rm eo} = \frac{2}{\pi^3\gamma}\int_0^\infty {\rm d}k \int_0^{2\pi} {\rm d}\phi \int_0^{2\pi} {\rm d}\theta k k'[k\cos\phi - k'\cos(\phi+\theta)] f_+(k)|U_{\rm eo}|^2.$$

In the above equations, $\gamma = \hbar v_F$; $k' = k + \hbar\omega_j/\gamma$; ω_j are the changes of the scattering frequencies; θ is the change of the scattering angle; $f_+(x)$ is the Fermi–Dirac function for electrons; n_e is the electron density in the graphene system; $U_{\rm ei}$, $U_{\rm ea}$, and $U_{\rm eo}$ are the scattering matrix elements which correspond to the interactions of the electrons with impurities, acoustic phonons, and optical phonons in graphene, respectively [16], $M_{\rm ei}$, $M_{\rm ea}$, and $M_{\rm eo}$ are the momentum transfer rates which correspond to the electron interactions with impurities, acoustic phonons, and optical phonons in graphene, respectively. Equation (1) implies that the momentum change of the electrons caused by the applied DC electric field has to be balanced owing to the scattering with impurities and phonons. Next, for the second moment, the energy-balance equation can be obtained for the electrons [14, 15]:

$$eF_x G = E_{\rm ea} + E_{\rm eo}, \tag{2}$$

where

$$G = \int_0^\infty {\rm d}k \int_0^\pi {\rm d}\phi \frac{f_+(k)k(k\cos\phi + k_v)}{\sqrt{k^2 + 2kk_v\cos\phi + k_v^2}},$$

$$E_{\rm ea} = -\frac{\hbar\omega}{\pi\gamma^2}\int_0^\infty {\rm d}k \int_0^{2\pi} {\rm d}\phi \int_0^{2\pi} {\rm d}\theta k k' f_+(k)|U_{\rm ea}|^2,$$

$$E_{\rm eo} = -\frac{\hbar\omega}{\pi\gamma^2}\int_0^\infty {\rm d}k \int_0^{2\pi} {\rm d}\phi \int_0^{2\pi} {\rm d}\theta k k' f_+(k)|U_{\rm eo}|^2,$$

$$k_v = k_F V_x/v_F,$$

V_x is the drift velocity of the electrons, ω is the phonon frequency, $E_{\rm ea}$ and $E_{\rm eo}$ are the energy transfer rates induced by the inelastic scatterings with acoustic and optical phonons, respectively, and G represents the energy integration. The energy balance equation implies that the energy gain of the carriers from the applied electric field has to be balanced with the energy loss caused by the scatterings with the phonons.

In a gated graphene sample, the majority of the charged impurities are located around the interface between the graphene layer and substrate with an effective impurity concentration [16]. Using the conventional random-phase approximation (RPA), the effect of the electron-electron screening can be included in the effective scattering in the graphene system. The inverse RPA screening length $\kappa_s = q_s[1 - \pi q/(8k_F)]$ is employed for the electron-impurity scatterings; $q_s = 4e^2k_F/(\kappa'\gamma)$, where κ' is the effective dielectric constant. The mismatch between the dielectric constants of the different material layers in the air-graphene-substrate system can be evaluated [17]. For the electron-acoustic phonon scat-

tering, we consider the deformation potential coupling between the electrons and longitudinal and transverse acoustic-phonon modes [12]. In this study, the inelastic nature of the electron-acoustic-phonon scattering is considered, in contrast to the usual quasi-elastic approximation for the electron-acoustic-phonon interactions. It is worth noting that in graphene, the optical phonon energy is relatively large. The acoustic-phonon scattering is more important for the transport coefficients in a graphene device [18]. The electron-optical-phonon interactions are considered using the conventional valence-force-field model for a graphene system [19]. At very high temperatures, the electrons interact strongly with the longitudinal and transverse optical phonons in graphene. These interactions cause a relatively large energy relaxation owing to the inelastic nature of the scattering.

We employ the drifted Fermi–Dirac function with an electron temperature of T_e as the distribution function for the electrons in graphene. Considering the law of charge number conservation, we obtain:

$$2(k_B T_e)^2 Li_2(-\mathrm{e}^{-\mu_e/(k_B T_e)}) + \pi\hbar^2 v_F^2 n_e = 0. \quad (3)$$

From this equation, we can obtain the chemical potential μ_e of the electrons in the presence of a DC electric field; $Li_n(x)$ is the complex poly-logarithm function. By solving Eqs. (1), (2), and (3) self-consistently, we obtain the drift velocity V_x, mobility μ of the electrons, and electron temperature T_e in the presence of the DC electric field F_x.

3 Results and discussion

Figure 2 shows the electron temperature T_e as a function of the electric field strength F_x for different electron densities, at a fixed lattice temperature of $T = 300$ K. In the presence of a weak electric field, T_e is approximately equal to the lattice temperature T in graphene. In other words, for weak electric fields, the electrons exhibit a linear response, where a heating of electrons does not occur. This implies that in graphene the Ohm's law is valid for weak electric fields. For strong electric fields, an electrons' heating occurs; the electron temperature T_e is higher than the lattice temperature T. The electron temperature rapidly increases with the strength of the electric field F_x, and a non-ohmic behavior can be observed. We revealed that the heating of the electrons depends strongly on the electron density in the graphene samples at a fixed F_x. A higher electron density leads to a stronger hot-electron effect. The temperature T_e of the hot electrons quasi-linearly depends on the electric field F_x.

Figure 3 shows the dependence of V_x as a function of F_x for different electron densities n_e, at a fixed lattice temperature T and impurity density in graphene. The V_x–F_x characteristic exhibits a distinct non-linear/non-ohmic behavior, in particular, for high electric fields. As expected, a larger F_x leads to a stronger non-linear/non-ohmic behavior. The very large electron velocities, up to 10^7 cm/s, emerge owing to the high mobility and high electron density. At high electric fields, the electron velocity in graphene does not completely saturate with the increase of the electric field F_x, up to 30 kV/cm. The origin of this phenomenon is that the energy gain of the electrons from the electric field is transferred to the acoustic phonons, owing to the interactions between the electrons and acoustic phonons. The optical phonon energy in graphene is ~ 196 meV. It is very challenging to observe the electron optical phonon scatterings, which is completely different from the behavior observed in conventional semiconductor devices. It is revealed that the electron velocity significantly depends on the elec-

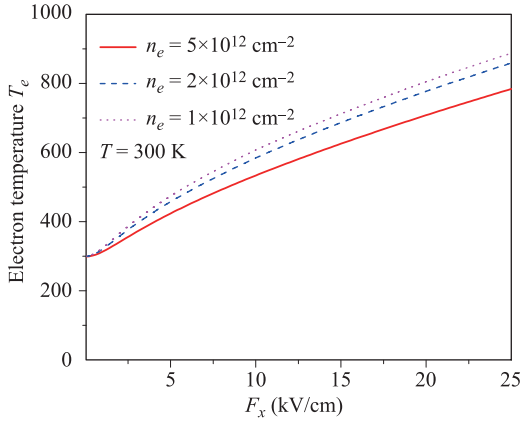

Fig. 2 Dependence of the electron temperature T_e as a function of the electric field strength F_x for different electron densities, at a fixed lattice temperature of $T = 300$ K.

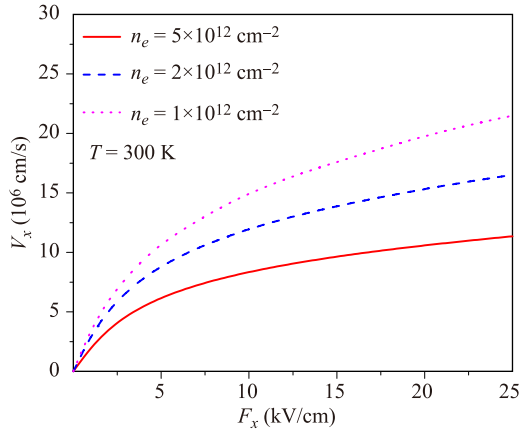

Fig. 3 Dependence of V_x as a function of F_x for different electron densities n_e, at a fixed lattice temperature T and fixed impurity density in graphene.

tron density. Moreover, the electron velocity increases with the electron density (or applied gate voltage V_g) in graphene. With the increase of the electron density, the non-linear/non-ohmic behavior of the V_x–F_x characteristic becomes more obvious. The acoustic-phonon scattering is relatively strong when F_x is not extremely high. Therefore, the strong interactions between the electrons and optical phonons occur mainly in the relatively strong field regime. The unique and important features of the strong-field electron transport in graphene can be understood mainly by analyzing the coupling between the electrons and acoustic phonons. These theoretical results are in agreement with the experimental observations [10, 11].

Figure 4 shows the electron mobilities μ as a function of the electric field F_x for different electron densities n_e, at a fixed lattice temperature T and impurity density. Our simulation results reveal a very high mobility in the considered system, up to 4000 cm/(V·s), even at room temperature. This shows that graphene can be employed to develop advanced nano-devices with high mobilities. Furthermore, the mobility decreases with the increase of the electric field F_x, as the high electric field leads to a strong scattering of the electrons. On the other hand, the electron temperature T_e increases with the electric field. One can obtain a high mobility by decreasing the electron density n_e. The carrier density can be effectively tuned through the gate voltage V_g. Therefore, the mobility in the considered graphene systems can be adjusted though the gate voltage V_g. Figure 5 shows the dependence of the electron mobility μ as a function of the electric field F_x for different temperatures T. It demonstrates that a significantly higher mobility can be achieved at lower temperatures, compared with the conventional semiconductor materials. These results show that the mobility increases with the decrease of the phonon temperature

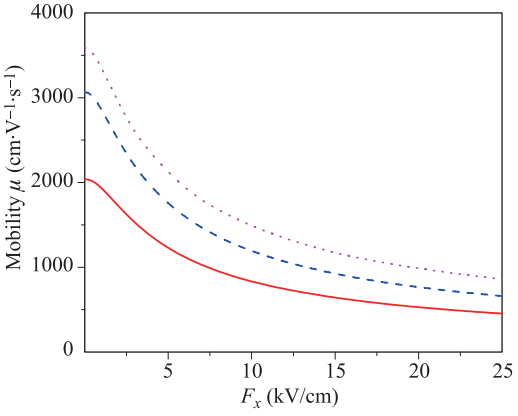

Fig. 4 Dependence of the electron mobility μ as a function of the electric field F_x for different electron densities n_e; the style of the curves and electron density values are equal to those in Fig. 3.

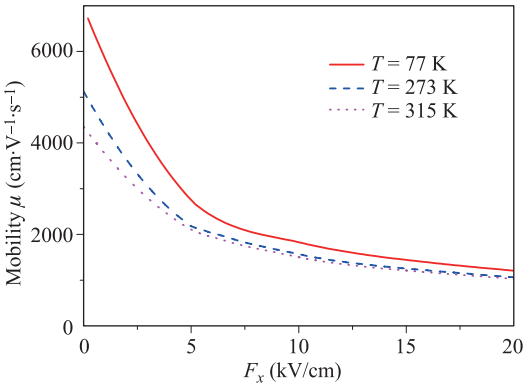

Fig. 5 Dependence of the electron mobility μ as a function of the electric field F_x for different temperatures T.

T, and it is sensitive to the temperature T. The electron scatterings with phonons become strong with the increase of the temperature T. The inelastic-electron-acoustic-phonon scattering is of key importance for the electric transport.

4 Conclusions

We theoretically studied the electron drift velocity and mobility of graphene by performing self-consistent calculations using the balance-equation approach. By considering the electron interactions with impurities, acoustic phonons, and optic phonons in a gated graphene-wafer system, we can summarize the following conclusions. The relationship between the electron drift velocity and DC electric field exhibited a distinctly nonlinear behavior. A very high electron velocity and mobility could be measured. In addition, we showed that the electron drift velocity saturation in graphene is incomplete. The electron drift velocity and electron temperature depended strongly on the electron density. The electron velocity increased with the decrease of the electron density (or applied gate voltage). We showed that a heating of the graphene carries can occur, while the temperature of the hot-electrons quasi-linearly depended on the electric field. The mobility increased with the decrease of the electron density. We showed that the mobility could be adjusted through the gate voltage. These theoretical findings are in a good agreement with the experimental observations. In addition to the experimental results, with this study, we further confirm that graphene can be utilized for high-field high-speed nano-electronic devices.

Acknowledgements This study was supported by the Fundamental Research Funds for the Central Universities (Grant No. 2015XKMS077) and the National Natural Science Foundation of China (Grant Nos. 11604380 and 11774416).

References

1. K. S. Novoselov, A. K. Geim, S. V. Morozov, D. Jiang, Y. Zhang, S. V. Dubonos, I. V. Grigoreva, and A. A. Firsov, Electric field effect in atomically thin carbon films, *Science* 306(5696), 666 (2004)
2. A. K. Geim and K. S. Novoselov, The rise of graphene, *Nat. Mater.* 6(3), 183 (2007)
3. K. I. Bolotin, K. J. Sikes, J. Hone, H. L. Stormer, and P. Kim, Temperature-dependent transport in suspended graphene, *Phys. Rev. Lett.* 101(9), 096802 (2008)
4. F. Xia, D. B. Farmer, Y. M. Lin, and P. Avouris, Graphene field-effect transistors with high on/off current ratio and large transport band gap at room temperature, *Nano Lett.* 10(2), 715 (2010)
5. G. Liu, W. Stillman, S. Rumyantsev, Q. Shao, M. Shur, and A. A. Balandin, Low-frequency electronic noise in the double-gate single-layer graphene transistors, *Appl. Phys. Lett.* 95(3), 033103 (2009)
6. L. M. Zhang and M. M. Fogler, Nonlinear screening and ballistic transport in a graphene p-n junction, *Phys. Rev. Lett.* 100(11), 116804 (2008)
7. Y. M. Lin, K. A. Jenkins, A. Valdes-Garcia, J. P. Small, D. B. Farmer, and P. Avouris, Operation of graphene transistors at Gigahertz frequencies, *Nano Lett.* 9(1), 422 (2009)
8. Y. Zhang and R. Tsu, Binding graphene sheets together using silicon: Graphene/silicon superlattice, *Nanoscale Res. Lett.* 5(5), 805 (2010)
9. T. J. Echtermeyer, M. C. Lemme, J. Bolten, M. Baus, M. Ramsteiner, and H. Kurz, Graphene field-effect devices, *Eur. Phys. J. Spec. Top.* 148(1), 19 (2007)
10. I. Meric, M. Y. Han, A. F. Young, B. Ozyilmaz, P. Kim, and K. L. Shepard, Current saturation in zero-bandgap, top-gated graphene field-effect transistors, *Nat. Nanotechnol.* 3(11), 654 (2008)
11. A. Barreiro, M. Lazzeri, J. Moser, F. Mauri, and A. Bachtold, Transport properties of graphene in the high-current limit, *Phys. Rev. Lett.* 103(7), 076601 (2009)
12. J. H. Chen, C. Jang, S. Xiao, M. Ishigami, and M. S. Fuhrer, Intrinsic and extrinsic performance limits of graphene devices on SiO_2, *Nat. Nanotechnol.* 3(4), 206 (2008)
13. X. F. Wang and T. Chakraborty, Collective excitations of Dirac electrons in a graphene layer with spin-orbit interactions, *Phys. Rev. B* 75(3), 033408 (2007)
14. X.-L. Lei, Balance Equation Approach to Electron Transport in Semiconductors, World Scientific, 2000
15. X. F. Zhao, J. Zhang, S. M. Chen, and W. Xu, Cerenkov acoustic-phonon emission generated electrically from a polar semiconductor, *J. Appl. Phys.* 105(10), 104514 (2009)
16. W. Xu, F. M. Peeters, and T. C. Lu, Dependence of resistivity on electron density and temperature in graphene, *Phys. Rev. B* 79(7), 073403 (2009)
17. H. M. Dong, W. Xu, Z. Zeng, T. C. Lu, and F. M. Peeters, Quantum and transport conductivities in monolayer graphene, *Phys. Rev. B* 77(23), 235402 (2008)
18. T. Stauber, N. M. R. Peres, and F. Guinea, Electronic transport in graphene: A semiclassical approach including midgap states, *Phys. Rev. B* 76(20), 205423 (2007)
19. W. K. Tse and S. S. Das, Phonon-induced many-body renormalization of the electronic properties of graphene, *Phys. Rev. Lett.* 99(23), 236802 (2007)